Scripta Materialia 167 (2019) 115–119

Contents lists available at ScienceDirect

Scripta Materialia

journal homepage: www.elsevier.com/locate/scriptamat

Elastic properties of the α' martensitic phase in the Ti-6Al-4V alloy obtained by additive manufacturing

Nathan Dumontet, Damien Connétable, Benoît Malard, Bernard Viguier *

CIRIMAT, Université de Toulouse, CNRS, INP- ENSIACET, 4 allée Emile Monso - BP44362, 31030 Toulouse Cedex 4, France

ARTICLE INFO

Article history:
Received 23 February 2018
Received in revised form 20 December 2018
Accepted 6 January 2019
Available online xxxx

Keywords:
Additive manufacturing
Titanium alloys
Elastic behaviour
Density functional theory (DFT)
Mechanical testing

ABSTRACT

Elastic behaviour of Ti-6Al-4V alloy elaborated through additive manufacturing process is studied both experimentally and trough atomistic simulation. By studying rough samples after fabrication and after heat treatment, the elastic properties of the α' martensitic phase is compared to that of α + β microstructure. Atomistic calculations were also performed on various super-cells varying their chemical composition in order to simulate α and α' phases and their full elastic stiffness tensors were determined. Both experimental and simulation results show that Young modulus of the α' phase is lower than that of α phase, while it presents a more anisotropic behaviour.

Additive manufacturing (AM) is widely used to elaborate industrial parts with an increasing variety of materials. In the present study, we focus on the titanium alloy Ti-6Al-4V elaborated by powder bed laser beam melting (PB-LBM). Ti-6Al-4V is a widely used Ti alloy known as an (α + β) alloy [1]. Indeed, wrought Ti-6Al-4V parts present a two phase microstructure with roughly 94% vol. for the hexagonal compact (hcp) α phase and 6% vol. for the body centred cubic (bcc) β phase [2]. When processed by AM, metallic alloys experiment a very high cooling rate that may result in out of equilibrium structure. For instance during PB-LBM processing of Ti-6Al-4V the cooling rate is in the range of 10^7–10^8 $K \cdot s^{-1}$ [3], resulting in a single phase α' martensitic structure [4,5]. This α' phase presents, similarly to the pure Ti-α phase, a hcp structure but it incorporates the alloying elements of the Ti-6Al-4V alloy and forms a very fine entangled needles microstructure [4,5]. Recent papers review the mechanical properties of the Ti-6Al-4V processed by AM [6,7]. These studies often focus on plastic properties and the low ductility of AM Ti-6Al-4V. In many instances the elastic behaviour of the martensitic α' is poorly documented. Few values of the Young modulus deduced from tensile testing are reported with quite a large scattering, the modulus varying from 94 to 118 GPa [6].

The purpose of the present study is to determine the elastic behaviour of the α' martensitic phase and compare it to that of the Ti-α phase. This is conducted in two complementary ways: i) by measuring experimentally the overall Young modulus of the α' phase on PB-LBM samples and ii) by calculating the elastic stiffness constants C_{ij} using atomistic simulations. The obtained results are discussed in regard to the literature data and an emphasis is placed on the evolution of elastic behaviour of the hexagonal phase when changing from pure Ti (α phase) to the martensitic phase α'.

In order to experimentally measure the Young modulus of the α' phase, samples were produced by PB-LBM in an M2 Cusing machine from Concept Laser, using Ti-6Al-4V powder with an average powder grain diameter of 35 μm. For tensile testing dog-bone plate shaped samples (2 mm thick, gage length with 2 mm width and 10 mm length) were manufactured. The surfaces of tensile specimens were ground using grade 600 SiC paper. For the resonance vibration measurements the samples are beam shaped with dimension 80 × 20 × 4 mm^3. Both types of sample were fabricated vertically, that is with the long axis of the specimen along the elaboration direction.

In most cases titanium pieces elaborated by PB-LBM are given an heat treatment (HT) in order to release residual stress and stabilise the microstructure by decomposing the α' martensite to the (α + β) microstructure [4]. This HT was applied using a Carbolite CWF 1300 under laboratory air, with a heating ramp 5 °C/min from room temperature up to 700 °C, holding 1 h at 700 °C and furnace cooling. It was verified by scanning electron microscopy observations that the microstructure of the raw AM samples consists of a unique hcp phase in the form of entangled fine needles, corresponding to the martensitic α' phase. The phase proportions were investigated by X-ray diffraction using a D8-2 diffractometer from Bruker with a Cu source and a 1D

* Corresponding author at: CIRIMAT, Université de Toulouse INP-ENSIACET, 4 Allée Emile Monso BP 44362, 31030 Toulouse, France.
E-mail addresses: nathan.dumontet@ensiacet.fr (N. Dumontet), damien.connetable@ensiacet.fr (D. Connétable), benoit.malard@ensiacet.fr (B. Malard), bernard.viguier@ensiacet.fr (B. Viguier).

https://doi.org/10.1016/j.scriptamat.2019.03.042
1359-6462/

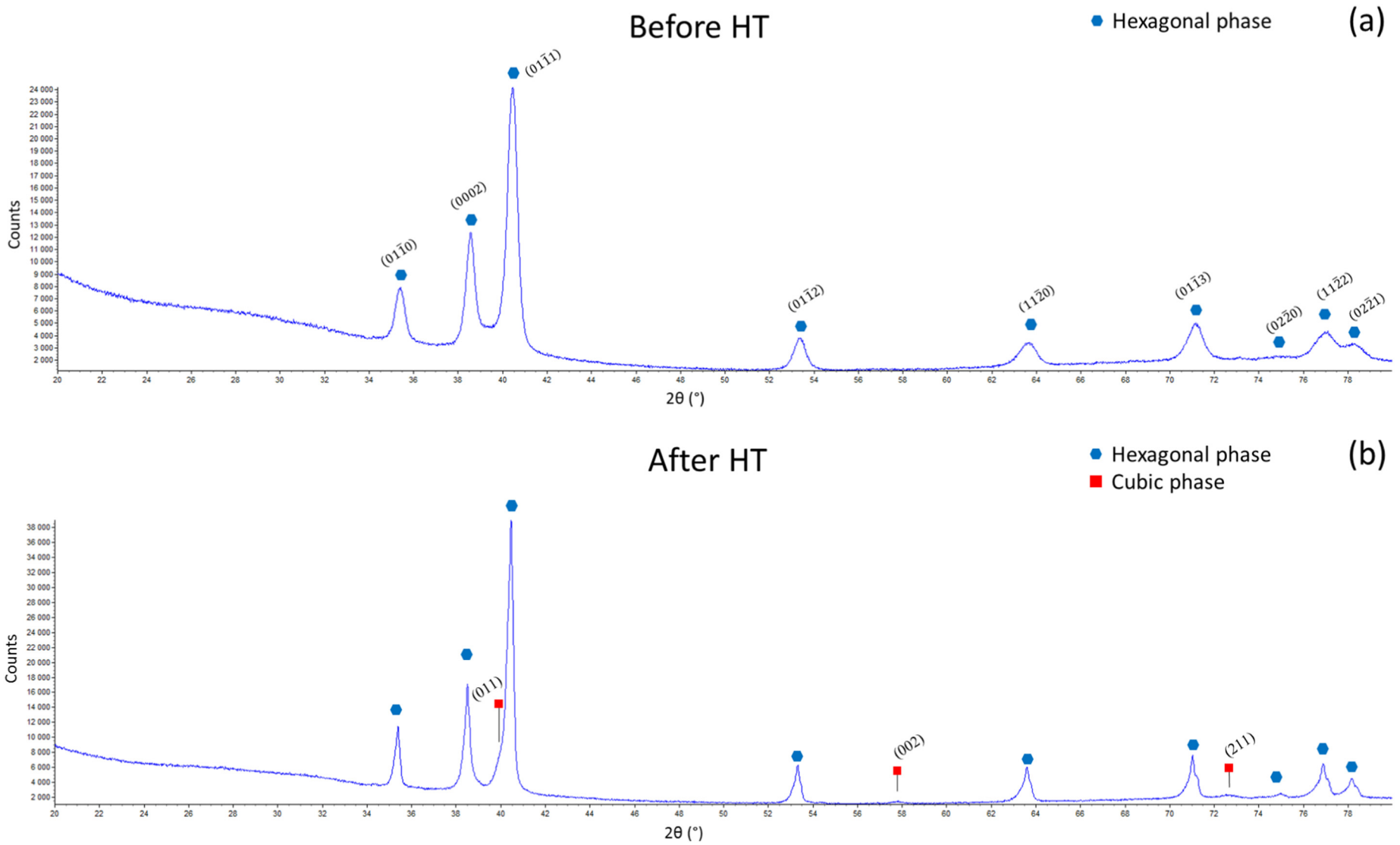

Fig. 1. X ray diffraction pattern on Ti-6Al-4V samples elaborated by AM a) in the raw fabrication state and b) after HT. The peak indexing of hexagonal (α' and α) and cubic (β) phases are showed.

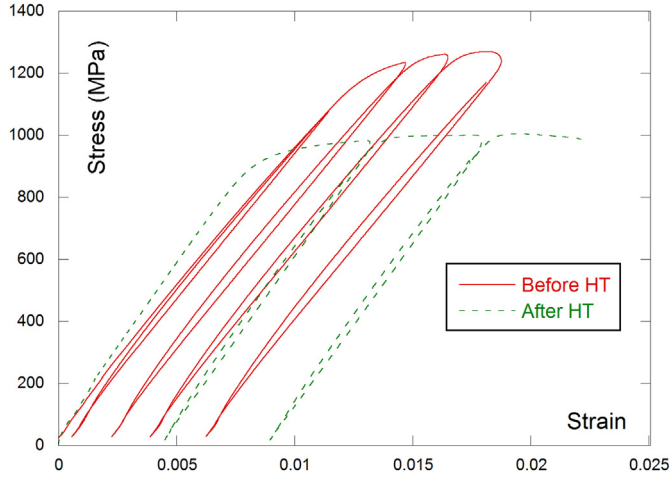

Fig. 2. Tensile curves used for measuring the Young modulus of the AM samples before and after HT.

LYNXEYE detector. Scans were performed from 20° to 80° by 0.02° steps every 3 s. The obtained diffractograms were analysed according to Rietveld technique using TOPAS 4.2 [8]. As can be seen in the Fig. 1(a) corresponding to raw AM sample, all the diffraction peaks observed are associated to a unique hcp phase with cell parameters: a = 292.9 pm and c = 465.5 pm. By contrast the diffraction pattern presented in Fig. 1(b) exhibits peaks from both the hexagonal α phase and the cubic β phase. This later accounts for 6% ±1% volume fraction. As a whole, we consider that the raw sample after AM is fully constituted by the α' martensitic phase, while after HT an (α + β) microstructure close to the equilibrium of the Ti-6Al-4V is present.

The tensile tests were performed at room temperature using a MTS Insight electrically driven tensile machine. The cross-head motion rate was fixed to 10^{-2} mm·s^{-1} and the elongation was measured using a MTS clip-on extensometer with initial spacing of 10 mm. Young modulus was also determined using impulse excitation technique, consisting in measuring the resonance vibration frequency of a beam under flexural vibration induced by a hammer hit. The device was installed in a furnace for measuring elastic properties during temperature cycles according to standardised methods [9]. During thermal cycling, heating rate was fixed to 5 °C/min and natural cooling in the furnace was used.

An example of room temperature tensile tests results is presented in Fig. 2 for the raw AM material and after HT. HT affects both elastic and plastic properties of Ti-6Al-4V. Indeed, the yield stress at 0.2% offset plastic strain decreases from 1172 MPa for the raw material down to 970 MPa after HT. Conversely, the elastic slope of the tensile curves increases after HT. Each sample was plastically deformed with imposed unloading – reloading cycles as can be seen in Fig. 2. The slope of the curve was measured on both loading and unloading elastic lines and the values were used to access the Young modulus. Two samples, labelled A and B, were both tested in the raw AM state and after HT. For each test 5 slopes were measured with very similar values, leading to a scattering of the Young modulus lower than 1.7 GPa for a given test. For both samples the Young modulus value increased after HT, evolving from 106 GPa in the raw AM state to 111 GPa after HT for sample A, respectively from 94 to 106 GPa for sample B. A similar scattering was also observed for the yield stress values between samples A and B. Those differences between samples are commonly observed in AM specimens as referred in the literature [10], this scattering may also be related to the quite small size of the gage length of the tensile sample used in the present study. The values of Young modulus of AM Ti-6Al-4V alloy measured by tensile testing in the present study in the raw fabrication state and after HT agree with previous results from the literature [11–13].

Table 1
Room temperature values of the Young modulus (in GPa) experimentally determined in the present study on Ti-6Al-4V AM sample before (α') and after (α + β) HT.

	Traction		Vibration	
Phases	Sample A	Sample B	Sample C	Sample D
Before HT (α')	106	94	98.4	98.7
After HT (α + β)	111	106	–	103.4

Resonance frequency measurements were performed during two thermal cycles on two different specimens labelled C and D. The first measurement performed on sample C, consists in heating to 400 °C, hold 5 min at this temperature and cooling. The Young modulus continuously measured along the thermal cycle is plotted in Fig. 3(a). The Young modulus decreases linearly with temperature, the value after thermal cycling (98.8 GPa) is very close from the initial value (97.9 GPa). This cycle allows determining the linear variation of the α' martensite Young modulus $E_{\alpha'}$ versus temperature (T) according to the relation:

$$E_{\alpha\prime}(GPa) = 99.8 - 0.0427 \times T\left(^{\circ}C\right). \quad (1)$$

A second measurement performed on sample D, consisted in heating the sample up to 700 °C, holding for 1 h and furnace cooling. This thermal cycle actually reproduces the HT performed on tensile sample as previously described. The evolution of Young modulus during this

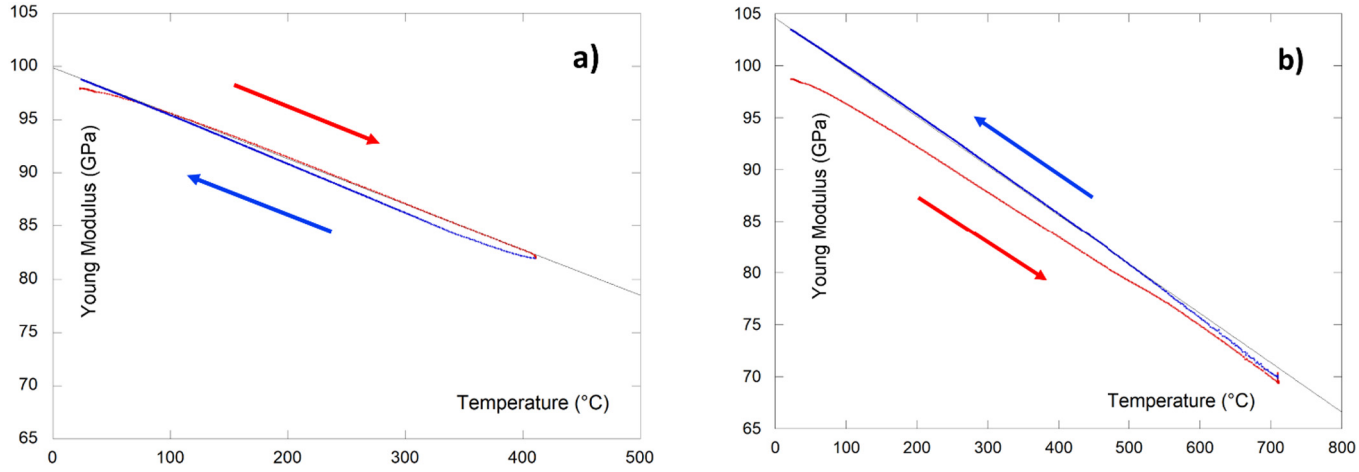

Fig. 3. Vibration measurement of Young modulus during heating and cooling cycle up to a) 400 °C and b) 700 °C.

Table 2
List of the five super-cells used for DFT simulations. The number of atoms is indicated together with the at.% of Al and V (in brackets). The cells Ti and Ti + 2Al + V represent the phases α and α' respectively.

	Phase	Ti	Al	V
Ti	α	24	0	0
Ti + Al		23	1 (4.2%)	0
Ti + V		23	0	1 (4.2%)
Ti + Al + V		22	1 (4.2%)	1 (4.2%)
Ti + 2Al + V	α'	21	2 (8.4%)	1 (4.2%)

cycle is plotted in Fig. 3(b). At the beginning of heating ramp, the Young modulus value (initial value 98.7 GPa) and its temperature dependence is very similar to that of sample C. For temperature over 500 °C, the variation of Young modulus deviates from linear temperature dependence. Upon cooling, some irreversible changes of the value of Young modulus and its slope versus temperature are observed. They are associated to the phase transition from α' to α + β. The cooling branch of the curve below 500 °C indicates a linear variation of (α + β) Young modulus $E_{\alpha+\beta}$ with T, according to the relation:

$$E_{\alpha+\beta}(GPa) = 104.6 - 0.0475 \times T\left(^{\circ}C\right). \quad (2)$$

The room temperature Young modulus of the sample D after HT is measured to be 103.4 GPa. Both this room temperature value and the temperature variation of Young modulus given by Eq. (2) are in quite good agreement with the values reported in the literature for elastic behaviour of wrought Ti-6Al-4V alloy [2,14].

A summary of the experimental results obtained in this part is given in Table 1 in which Young modulus values for samples before and after HT are compiled. Despite the absolute values obtained and their scattering depend on the experimental technique, both tensile testing and vibration technique clearly indicate that the Young modulus of the α' martensite is lower than that of (α + β) microstructure for the Ti-6Al-4V alloy. Moreover it is recognized that vibrational method are more accurate than tensile tests for measuring Young modulus of metallic materials, see e.g. [15]. This method allowed to measure the temperature variation of the α' martensite Young modulus which has never been reported in the literature to our knowledge.

The Young modulus of the α phase is even higher than that of (α + β) microstructure, due to the fact that the β phase has a low Young modulus [2]. Consistently the Young modulus of pure titanium α phase was reported to be 112 GPa [2,16]. Which means that the martensitic α' phase may present a Young modulus significantly lower than that of the α phase.

Atomistic calculations were performed with the density functional theory (DFT) using Vienna ab initio Simulation Package [17]. Self-consistent Kohn-Sham equations were solved using the projector augmented wave pseudo-potentials [18]. We used the Perdew-Burke-Ernzerhof [19] exchange and correlation functional. The plane-wave energy cut-off was set to 500 eV. Equivalent Γ-centred 40x40x40 Monkhorst-Pack meshes [20] were used to sample the first Brillouin zone of the primitive cell (by using a band folding approach with two atoms per unit cell).

Table 3
Result of DFT calculations for the five super-cells considered. The stiffness tensor components are given in GPa and cell parameters are given in pm.

	C_{11}	C_{12}	C_{13}	C_{33}	C_{44}	C_{66}	a	c
Ti	178.4	80.9	76.9	189.2	43.4	48.8	293.7	464.8
Ti + Al	174.5	83.9	73.6	188.0	45.2	45.3	292.7	467.9
Ti + V	163.0	98.3	79.5	191.0	36.3	32.4	292.6	464.2
Ti + Al + V	162.9	100.9	77.4	193.2	40.8	31.0	291.8	463.8
Ti + 2Al + V	161.0	104.3	75.8	198.6	43.0	28.4	291.2	464.1

Table 4
Stiffness tensor, in GPa, from the literature for pure Ti and substituted (3 at.%) cells.

		C_{11}	C_{12}	C_{13}	C_{33}	C_{44}	C_{66}
Experimental [16]	Ti	160.0	90.0	72.3	183.0	45.0	35.0
Simulation [22]	Ti	175.0	89.0	84.0	192.0	45.0	43.0
	Ti + Al	171.9	94.1	84.1	190.6	39.2	38.9
	Ti + V	164.8	99.8	86.4	191.0	30.2	32.5

To perform elastic calculations, we choose five different types of strain to compute the five independent elastic constants. The elastic energy U is approximated by a quadratic function of the strain components (see [21]) as described with more details in supplementary data file (available on line).

A super-cell approach was used with full periodic boundary conditions to describe substituted systems. The super-cell is based on the crystallographic structure of pure titanium α phase, space group $P6_3/mmc$ where titanium (Ti) atoms occupy the positions 2c. In order to simulate alloys, vanadium (V) and/or aluminium (Al) atoms have been substituted to Ti atoms in the super-cell. For the super-cells containing several added elements in substitution at the same time, we considered different cases where the substituted atoms were either in first (1NN) or in second-nearest neighbouring positions (2NN). We found that Al-V interaction is attractive at short range (binding energy is equal to about 20 meV), alloying atoms were thus placed in 1NN positions in our simulations. Five different super-cells were used, as shown in Table 2, with an increasing number of substitution atoms, in order to study the evolution of properties from the pure Ti super-cell to the Ti + 2Al + 1 V super-cell. This latter represents the martensitic α' phase, the current chemical composition being 4.9 wt% Al and 4.6 wt% V quite close to the Ti-6Al-4V alloy composition.

From these simulation results shown in Table 3, one can see that varying the chemical content of the super-cell has a main effect on the values of C_{11} and C_{33}. Adding alloying elements V and Al lowers the value of C_{11} and rises C_{33}. For the pure Ti-α phase, the C_{ij} values obtained, Table 3, are well in line with the C_{ij} experimental values reported in the literature [16] and presented in Table 4. DFT calculations of the C_{ij} were previously performed by Wilson et al. [22] for pure Ti and with the incorporation of various substitutional elements. These authors also showed that different alloying elements have different effects on the various components of the stiffness tensor. However, they limited their calculations to a lower amount (3 at.%) of substitutional atoms and did not study the combination effect observed when alloying

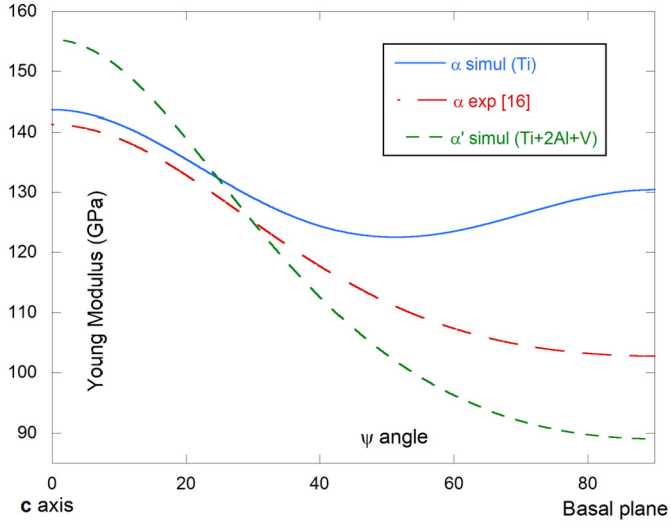

Fig. 4. Young modulus along a direction inclined by the angle ψ with respect to the **c** axis of the hexagonal structure.

Table 5
Average Young modulus from experimental and simulation determination for both α and α' phases. Values are deduced from the present study except for the α experimental [16].

E_{Hill} (GPa)	Experimental	Simulation
α	112.5	125.4
α'	98.5	105.0

with both V and Al in order to get closer to the composition of the α' martensite phase.

The increasing difference between components C_{11} and C_{33} that is observed in Table 3 with the incorporation of alloying elements Al and V, reveals an increased anisotropic character of the elastic behaviour of the hcp phase when changing from α to α' phase. This is better represented by calculating the Young modulus along a direction with increasing inclination with respect to the **c** axis, represented by the angle ψ. Young modulus versus the ψ angle are displayed in Fig. 4 where the experimental values come from Ogi et al. [16] and simulation data from this work. It appears that Young modulus is maximum along the **c** axis, minimum in the basal plane (Young modulus is isotropic in basal plane for the hexagonal system) for Ti + 2Al + 1 V simulation (α' phase) and for the experimental values of the α phase. The phase with the higher anisotropy is the α' martensite with values of $E(\psi = 0°) = 155$ GPa and $E(\psi = 90°) = 89$ GPa.

Finally, it is interesting to compare the average value of the Young modulus for hcp phases α and α'. Some values presented in Table 5 are calculated from C_{ij} through Hill averaging between Voigt and Reuss modulus [23]. C_{ij} values from simulation in the present study are used for both α and α' phases, while experimental values of C_{ij} are taken from [16] for Ti-α phase. The experimental value for the α' phase is taken from vibrational technique presented in this paper (Table 1). One can see comparing the values in Table 5 that for both phases experimental values are lower than calculated ones, however both experiment and simulation indicate similar variation from α' phase to α phase. It is also confirmed that the Young modulus of the martensitic phase α' is lower than that of the pure Ti-α phase.

To summarise, the elasticity of the α' martensitic phase of the Ti-6Al-4V alloy obtained by PB-LBM AM has been investigated using two experimental methods and DFT simulations. For the first time, the temperature dependence of the Young modulus was determined using vibrational techniques, before and after HT, corresponding to the α' and the (α + β) microstructures. It is shown that the Young modulus of the martensitic phase is lower than that of the pure Ti-α phase. DFT calculations showed the influence of Al and V substitutional elements on the elastic constants of the hexagonal phase. Stiffness tensors of super-cells representing α and α' phases were calculated. The values confirmed the lower value of Young modulus for the martensitic α' phase and also showed that its elastic behaviour is more anisotropic than that of the α phase.

Acknowledgements

F. Galliano from the company MBDA is gratefully acknowledged for providing additive manufactured specimens. The Institut Carnot 'Chimie Balard Cirimat' (ANR Program) is acknowledged for founding this study.

Appendix A. Supplementary data

Supplementary data to this article can be found online at https://doi.org/10.1016/j.dummy.2019.01.002.

References

[1] G. Lutjering, J.C. Williams, Titanium, Ed. Springer, 2003.
[2] R.F. Boyer, E. Collings, Materials Properties Handbook: Titanium Alloys, ASM international, 1994.
[3] B. Vrancken, V. Cain, R. Knutsen, J. Van Humbeeck, Scr. Mater. 87 (2014) 29–32.
[4] J. Yang, H. Yu, J. Yin, M. Gao, Z. Wang, X. Zeng, Mater. Des. 108 (2016) 308–318.
[5] T. Vilaro, C. Colin, J.D. Bartout, Metall. Mater. Trans. A 42 (2011) 3190–3199.
[6] A.M. Beese, B.E. Carroll, JOM 68 (2016) 724–734.
[7] H. Shipley, D. McDonnell, M. Culleton, R. Coull, R. Lupoi, G. O'Donnell, D. Trimble, Int. J. Mach. Tools Manuf. 128 (2018) *128*, 1–20.
[8] A.A. Coelho, J. Appl. Crystallogr. 51 (2018) 210–218.
[9] Standard Test Method for Dynamic Young's Modulus, Shear Modulus, and Poisson's Ratio by Impulse Excitation of Vibration, ASTM Standart E1876–09.
[10] W. Xu, M. Brandt, S. Sun, J. Elambasseril, Q. Liu, Acta Mater. 85 (2015) 74–84.
[11] L. Facchini, E. Magalini, P. Robotti, A. Molinari, S. Höges, K. Wissenbach, Rapid Prototyp. J. 16 (2010) 450–459.
[12] B. Vrancken, L. Thijs, J.-P. Kruth, J. Van Humbeeck, J. Alloys Compd. 541 (2012) 177–185.
[13] J. He, D. Li, W. Jiang, L. Ke, G. Qin, Y. Ye, D. Qiu, Materials 12 (2019) 321.
[14] Y.T. Lee, G. Welsch, Mater. Sci. Eng. A 128 (1990) 77–89.
[15] B.A. Latella, S.R. Humphries, Scr. Mater. 51 (2004) 635–639.
[16] H. Ogi, S. Kai, H. Ledbetter, R. Tarumi, M. Hirao, K. Takashima, Acta Mater. 52 (2004) 2075–2080.
[17] G. Kresse, J. Hafner, Phys. Rev. B 47 (1993) 558–561.
[18] G. Kresse, D. Joubert, Phys. Rev. B 59 (1999) 1758–1775.
[19] J.P. Perdew, K. Burke, M. Ernzerhof, Phys. Rev. Lett. 77 (1996) 3865.
[20] H.J. Monkhorst, J.D. Pack, Phys. Rev. B 13 (1976) 5188–5192.
[21] V. Trinite, Etude théorique des phases du titane, PhD Thesis, Ecole Polytechnique, Paris, 2006.
[22] N.C. Wilson, K. McGregor, M.A. Gibson, S.P. Russo, Modelling Simul. Mater. Sci. Eng. 23 (2015), 015005.
[23] R. Hill, Proc. Phys. Soc. A 65 (1952) 349.